Contents lists available at ScienceDirect

Arabian Journal of Chemistry

journal homepage: www.ksu.edu.sa

Original article

Study on preparation and performance of bagasse/sodium carboxymethyl cellulose gel for inhibiting coal spontaneous combustion

Xiaowei Geng [a,c], Yuanyuan Feng [a], Yinhui Wang [b,d], Hemeng Zhang [a,c], Yujiao Liu [a,c], Ke Gao [a,c,e,*]

[a] College of Safety Science and Engineering, Liaoning Technical University, Huludao, Liaoning 125105, China
[b] State Key Laboratory of Coal Mine Disaster Prevention and Control, Fushun, Liaoning 113122, China
[c] Key Laboratory of Mine Thermodynamic Disasters and Control of Ministry of Education, Liaoning Technical University, Huludao, Liaoning 125105, China
[d] Shenyang Research Institute, China Coal Technology & Engineering Group, Shenfu Demonstration Zone, Liaoning 113122, China
[e] Ordos Institute of Liaoning Technical University, Ordos 017004, China

ARTICLE INFO

Keywords:
Coal spontaneous combustion
Gel
Bagasse
Sodium carboxymethyl cellulose

ABSTRACT

In order to effectively prevent and control coal spontaneous combustion and improve the safety of coal mining, bagasse carboxymethy cellulose (BCC) prepared from bagasse (BS) and sodium carboxymethyl cellulose (CMC) were used as the substrates. A gel (BCC-CMC) for inhibiting coal spontaneous combustion was prepared using a chemical crosslinking method involving zirconium citrate crosslinking and glucono-delta-lactone (GDL) modification. X-ray diffraction (XRD) and Fourier transform infrared (FTIR) spectroscopy were utilized to characterize both the crystal and molecular structure of bagasse and its derived bagasse carboxymethyl cellulose. The results indicated that new carboxymethyl groups were introduced into bagasse during the treatment, facilitating the successful extraction and preparation of sodium carboxymethyl cellulose. The results of viscosity and bonding tests demonstrated that the concentration and dosage of CMC had the most significant influence on the gel viscosity, which remained higher and more stable at room temperature. The coal bonded by the gel coal mixture can effectively seal surface cracks, with a bonding degree of up to 70.72 %. TG-DTG, temperature-programmed oxidation experiment and FTIR analyses revealed that, compared to raw coal, coal samples treated with gel exhibited improved stability, fewer active groups, and fewer oxygen-containing functional groups, effectively inhibiting coal's low temperature oxidation and reducing the risk of spontaneous combustion. The gel is environmentally friendly, cost-effective, and exhibits good flame retardant properties. This study is of great significance for preventing and controlling coal spontaneous combustion, effectively ensuring the safe production of coal resources and the safety of mine workers, achieving the green sustainable development of the mine.

1. Introduction

Coal, as a significant energy source in the energy structure, plays a leading role in economic development (Yuan et al., 2023). With the increase of mining, and the improvement of gas extraction intensity, the residual coal in goaf increases, and the air leakage phenomenon is serious (Ding et al., 2023; Gao et al., 2022). Therefore, with the increase of underground coal and rock disasters, the risk of coal spontaneous combustion is also increasing (Qiao et al., 2022; Shi et al., 2024). Currently, over half of China's major coal mines are at risk of spontaneous combustion, with coal-induced fires constituting over 85 % of all mine fires (Zhu et al., 2020). Coal spontaneous combustion results in coal resources wastage, environmental pollution, and potentially immeasurable casualties or property damage, significantly jeopardizing employee safety and enterprises productivity (Deng et al., 2022; Jia et al., 2024). Therefore, developing a clean and efficient anti-coal spontaneous combustion material is necessary.

Commonly employed methods for preventing coal spontaneous combustion include grouting (Wang et al., 2019), inert gas injection (Si et al., 2024), inhibitor (Huang et al., 2022), pressure equalization fire prevention and extinguishing technology (Ren et al., 2016), gel (Ren et al., 2020), gel foam (Guo et al., 2019), etc. Among them, in grouting technology, the slurry material is easy to separate from water, and can only flow along the low stratum, which is easy to form a blind spot for

* Corresponding author at: College of Safety Science and Engineering, Liaoning Technical University, Huludao, Liaoning 125105, China.
E-mail address: gaoke@lntu.edu.cn (K. Gao).

https://doi.org/10.1016/j.arabjc.2024.105991
Received 18 May 2024; Accepted 10 September 2024
Available online 26 September 2024

treatment. Inert gas has a high cost, and requires a high degree of on-site sealing. Physical inhibitors contain corrosive, and chemical inhibitors are expensive, so they cannot be used on a large scale. The requirements of pressure equalizing fire prevention and extinguishing are strict, and the scope of action is limited, which has little preventive effect on the top, upper layered goaf and coal pillar. The three-phase foam is dried and pulverized after losing water, which leads to the inability to completely cover coal. Organic curing foam is seriously polluted; Inorganic cured foam has poor fluidity. Gel is widely utilized due to its excellent water retention, stability and plugging ability, simple production process and low cost. At present, the commonly used mine fire prevention gel are divided into inorganic gels and organic gels. The most widely used inorganic gels are silicate gels, which are thermally stable and have a simple process, but produces toxic and harmful gases such as NH_3 during the gel formation process (Wang et al., 2016; Li et al., 2019), polluting the working environment. Organic gels are mainly composed of hydrophilic polymers, including natural polymers such as cellulose, protein, gelatin, synthetic and modified cellulose, xanthan gum, which have good plugging and temperature reduction properties. Sodium carboxymethyl cellulose (CMC) exhibits strong water absorption owing to the abundance of hydrophilic groups, including hydroxyl and carboxyl groups along its molecular chain. Due to its biocompatibility, low cost, environmental friendliness, and non-toxicity nature, CMC finds widespread application in chemical industry, construction, medicine, papermaking and other fields (Markeb et al., 2023; Kim et al., 2023; Wang and Shi, 2022). The gel prepared by graft copolymerization with CMC as matrix has high water absorption, strong fire resistance, good thermal stability and better fire prevention and extinguishing effect (Li, 2018; Li et al., 2019). Polymer solution needs to react with crosslinking agent to form solution. Generally, high-valent metal ions are used as crosslinking agent and carboxylic acid compounds are used as chelating agents. PVA-CMC-attapulgite composite membranes crosslinked by citric acid can be used as a wound dressing with biological properties (Farid et al., 2022). CMC was extracted from filter paper and crosslinked it with $AlCl_3{\cdot}6H_2O$ to obtain CMC gels with enhanced water absorption and retention properties (Ma and Miao, 2023). The gel prepared with CMC as matrix and Al^{3+} as crosslinking agent has strong water absorption and is an ideal fire extinguishing material (Liu et al., 2021). Demonstrating that the plugging ability of the dual network gels was superior that of CMC single network gels (Chen and Zhou, 2023). The gels by combining zirconium citrate, and glucono-delta-lactone (GDL) with CMC, has good solidification and thermal stability, and their addition inhibited the coal oxidation reaction (Dong et al., 2020; Wang et al., 2020). From the above literature, it is evident that CMC-based gels exhibit good thermal stability and a simple preparation process; however, resource reuse is not achieved.

Cellulose, as an abundant global resource, is derived from various sources including bagasse, straw, cotton stalks, etc. The gels prepared from sago pith waste and bagasse had better adsorption capacity and thermal stability (Fan et al., 2020; Beh et al., 2020). Cellulose is difficult to dissolve in common solvents. Alkali/urea low-temperature solvent can improve the solubility and stability of cellulose solution, which greatly improves the functional utilization of bagasse cellulose. Using bagasse as raw material, bagasse cellulose was extracted after acid-base/urea treatment, and the prepared gel had high adsorption and water absorption (Chang et al., 2024; Rong et al., 2022). The gel prepared by mixing alkali/urea treated bagasse cellulose with CMC, exhibited higher swelling rates with adjustments in the ratio of bagasse cellulose to CMC (Zeng et al., 2019). The literature indicates that cellulose-based biomass hydrogels have a broad range of applications due to their simple preparation process, low cost, and potential for waste utilization. Sugarcane, being an important crop, holds important economic value. Bagasse primarily comprises elements such as C, H, O, N, and S, with its constituents consisting mainly of cellulose, hemicellulose, lignin, and extracts, rendering it suitable for biomass gels. Sugarcane bagasse ash has a relatively stable chemical composition and it's an effective supplementary cementitious material (SCM) (Zhang et al., 2020). Utilizing bagasse, abundant in source, as a raw material can reduce costs and facilitate effective waste utilization, contributing to sustainable development. The development of new materials for biomass gels significantly influences the advancement of a low-carbon economy.

From the above studies, it can be found that there are many studies on sodium carboxymethyl cellulose gels for coal mining, but CMC produces odor during dissolution by heating. Although most studies on bagasse-based gels focus on swelling and adsorption properties, few investigate adhesion and flame retardant properties. Therefore, this paper employs bagasse (BS) and CMC as raw materials. The bagasse carboxymethyl cellulose (BCC), proposed to be derived from bagasse, were blended with CMC. Zirconium citrate served as the crosslinking agent to from BCC/CMC composite hydrogels, and the adhesion and flame retardant properties of the hydrogels were experimentally evaluated.

2. Materials and methods

2.1. Experimental materials and instruments

Sugarcane bagasse (BS), an herbaceous plant with thick, cellulose-rich stems, was purchased from Guangdong, China, and sodium carboxymethyl cellulose (CMC, CP), was purchased from Sinopharm Chemical Reagent Co. Ltd. (Shanghai, China), which are the basic materials for the preparation of gels. Catechol oxidase, glucose oxidase and sodium carbonate (Na_2CO_3, AR) were purchased from Hefei Bomei Biotechnology Co., Ltd. Sodium silicate (AR), sodium bicarbonate ($NaHCO_3$, AR), and chloroacetic acid (AR) were purchased from Sinopharm Chemical Reagent Co., Ltd. (Shanghai, China). Tween-80 (CP), magnesium sulfate ($MgSO_4$, AR), and methanol (AR) were purchased from Tianjin Xinbote Chemical Co., Ltd. These substances modified BS to bagasse carboxymethyl cellulose (BCC). Citric acid (CA, AR) was purchased from Tianjin New Technology Industrial Park Kemao Chemical Reagent Co., Ltd, zirconium tetrachloride ($ZrCl_4$) was purchased from Sinopharm Chemical Reagent Co., Ltd. (Shanghai, China), and glucono-delta-lactone (GDL) was purchased from Hefei Bomei Biotechnology Co., Ltd. Among them, CA and $ZrCl_4$ formed the cross-linking agent, and GDL was used as the pH adjusting agent during gel formation. Sodium hydroxide (NaOH, AR), as an acid neutralizer, was purchased from Tianjin Beilian Fine Chemicals Development Co., Ltd. Among them, AR is analytical reagent, CP is chemical pure. Deionized water, from a laboratory ultrapure water apparatus. The raw coal samples is the anthracite obtained from Zhaogu, China. The coal is pulverized using a ball-mill and passed through a 60-mesh sieve, and then loaded into the system for testing. The results of the proximate and ultimate analyses of the raw coal samples are shown in Table 1.

The main instruments used comprised an electronic balance (FB204C, Shanghai Youke Instrumentation Co., Ltd., China), magnetic stirrer (85-2, Changzhou Yuexin Instrument Manufacturing Co., Ltd., China), digital thermostatic water bath (HH-4, Changzhou Jiangnan Experimental Instrument Factory, China), constant temperature glass water bath (SYP, Changzhou Mengte Instrument Manufacturing Co., Ltd., China), drying oven(DZF-6020A, Beijing Zhongxingweiye Instrument Co., Ltd., China), NDJ-8T viscometer (Shanghai Lichen Instrument Technology Co., Ltd., China), X-ray diffractometer (Rigaku SmartLab SE, Japan), Thermogravimetric analyzer (Netzsch STA 449 F3, Germany), and Fourier infrared spectrometer (Nicolet iS 10, America).

2.2. Preparation process of BCC-CMC gels

BS was screened, dried, dusted to remove impurities, and crushed to 120~150 mesh size. Subsequently, 2 kg of bagasse powder was placed in a container, and 10 kg of water was added to prepare a bagasse solution. After mixing catechol oxidase, glucose oxidase, Na_2CO_3, Tween-80, water, 2 g of the resulting mixture was added to the bagasse solution.

Table 1
Proximate and ultimate analyses of the raw coal samples.

Raw coal samples	Proximate analysis, mass%				Ultimate analysis, mass%,				
	M_{ad}	A_{ad}	V_{ad}	FC_{ad}	C	H	O	N	S
Raw coal samples	1.11	14.11	6.44	78.34	80.91	2.224	4.467	0.73	0.837

M_{ad}: moisture content; A_{ad}: ash content; V_{ad}: volatile content; FC_{ad}, fixed carbon content.

The mixture was stirred and left, at room temperature for 4 h, filtered it to remove impurities, dehydrated and dried to obtain bagasse cellulose (BSC). Chloroacetic acid, sodium silicate, $MgSO_4$, $NaHCO_3$ and the prepared 40 % NaOH solution were mixed thoroughly and added to a container containing the prepared bagasse cellulose. The reaction was carried out in a constant temperature water bath at 30 °C for 30 min, followed by stirring at 60 °C for 1 h using a magnetic stirrer. After cooling to room temperature, it was washed with 80 % methanol, centrifuged and dried to obtain BCC (Wang, 2018).

The crosslinking agent comprises a mixture of $ZrCl_4$ and CA. Firstly, prepare a $ZrCl_4$ solution with a mass fraction of 20 %. Add CA to the solution, with the mass of $ZrCl_4$ being twice times of that of CA. Stirred to form the zirconium citrate solution. Next, titrate the solution with 5 % NaOH while monitoring the pH value with pH test paper and pH meter, and white precipitates will appear during the titration (Dong et al., 2020). Since pH affects the dissociation rate of Zr^{4+} in the crosslinking agent. Cease titration when the pH value reaches approximately 6.5~7 (Dong et al., 2022; Wang et al., 2023; Zhao, 2022), then allow solution to clarify. The upper layer of the clarified solution constitutes the desired crosslinking agent. Mix the BCC solution with the CMC solution in the ratio of 1:2 and stir thoroughly. Subsequently, add the zirconium citrate solution and GDL solution dropwise. After thorough stirring, the gel forms. Among them, the concentration of BCC-CMC solution is 2 %, 2.5 % and 3 %, the concentration of zirconium citrate solution is 20 % and 30 %, and the dosage is 5 %, 8 % and 10 % of BCC-CMC solution. The concentration of GDL is 1.5 %, 2 % and 2.5 %, and the dosage is 1.5 %, 2 % and 2.5 % of the BCC-CMC solution. The gel formation and the experimental procedure are shown in Fig. 1 and Fig. 2.

2.3. Performance test of BCC-CMC gels

2.3.1. Gelation time test

The gelation time was determined using the drip timing method. Take 20 mL of the thoroughly mixed gel solution and pour it into a beaker through a funnel. Record the time when the first drip occurs. Repeat this process every 3 min until the interval between consecutive drip exceeds 1.5 times that of the previous one, then discontinue drip (Wang et al., 2020). The gelation time is defined as the duration from the first drip to the current drip.

2.3.2. Bonding test

The prepared gel was uniformly mixed with 40~60 mesh coal samples, the weight of the coal sample is M_1, with a coal-to-gel ratio of 10:1. After thoroughly mixing and drying the gel with the coal samples, the mixture was sieved, and the weight of the bonded coal remaining on the screen, M_2, was measured. The formula for calculating the bonding rate is as follows:

$$k = M_2/M_1 \quad (1)$$

Where k is for the bonding ratio, M_1 is for the 40~60 mesh coal samples, g. M_2 is for bonded coal remaining on the screen, g.

2.3.3. Viscosity test

The prepared gel was transferred into a beaker, and a touch screen rotational viscometer LC-NDJ-8 T equipped with a uniform rotor was utilized to measure the change in gel viscosity over, time and observe its stability. Starting from the gel preparation, the viscosity measurements were initially taken at 4-minute intervals, then at 2-minute intervals up to 16 min, followed by viscosity testing after 12 h and 24 h.

2.3.4. X-ray diffraction (XRD) experiment

X-ray diffraction technique is employed to analyze the crystal structure of cellulose, resulting in distinct diffraction patterns for each sample. The crystal structures of dried and crushed BS, BCC, and BSC were characterized using an X-ray diffractometer (model: Rigaku SmartLab SE, Japan) equipped with a Cu target. Diffraction intensities were measured within a 2θ angle range of 5° to 65° at a rate of 2° per minute.

2.3.5. Thermal analysis

The prepared gel was dried in a vacuum drying oven, and 10 mg was put into a thermogravimetric analyzer after grinding to analyze the thermal stability and thermal decomposition of the gel. In this experiment, the heating rate was set at 10 °C/min, the heating range is 30~800 °C, and the atmosphere was nitrogen.

The thermal analysis of the gel was assessed using the NETZSCH Thermogravimetric Analyzer from Germany. Anthracite coal was chosen as the coal sample, with 10 mg of 80~120 mesh coal evenly placed into the crucible. The temperature was then increased from 30 °C to 800 °C at a rate of 10 °C/min under a nitrogen protective atmosphere. Subsequently, 1 mg of gel was mixed with 10 mg of coal. This process was repeated for comparative experiments between raw coal and coal-gel mixtures to analyze the gel's impact on the coal's spontaneous combustion process by comparing changes in mass and heat during the coal heating process.

2.3.6. Functional groups test

Fourier Transform Infrared Spectroscopy (FTIR) was employed to

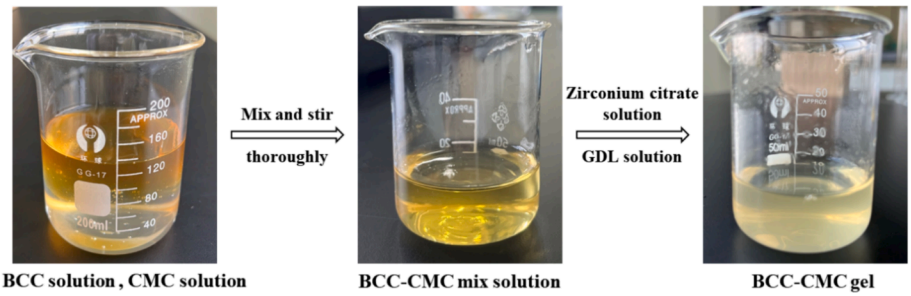

Fig. 1. Gel formation process.

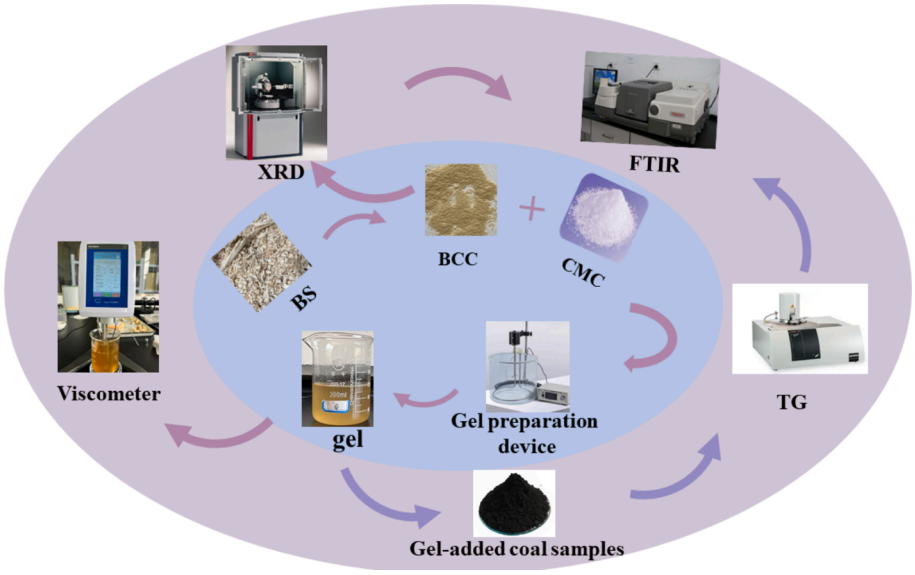

Fig. 2. Experimental process.

analyze the functional groups in bagasse samples and assess the effect of the gel on the microstructure of the coal samples, thus examining its effect of the gel on the spontaneous combustion process of coal. The scanning range was set from 4000 cm^{-1}~500 cm^{-1} with a resolution of 4 cm^{-1}, and the scanning rate was 64 scans per second.

2.3.7. Determination of the properties of BCC-CMC gel to inhibit the temperature-programmed oxidation of coal

The coal sample used in the experiment were Zhaogu anthracite. Each per portion raw coal was divided into 50 g and placed in a sealed bag for backup. The raw coal sample and the prepared gel were stirred evenly in the ratio of 5: 1, sealed and placed at room temperature, dried in a vacuum drying oven at 40 °C for 24 h, taken out. The coal sample was crushed and ground to a particle size range of 60~80 mesh by a coal mill. The raw coal sample and the gel-added coal sample were loaded into the coal sample tank respectively, and the inhibition rate test was carried out during the programmed temperature rise. The measurement parameters were as follows: the initial temperature of the test furnace was set at 30 °C, the termination temperature was set at 250 °C, and the heating rate was set at 1 °C/min. The air flow rate was 100 mL/min. The coal sample tank were cylindrical. During the experiment, the coal sample tank were placed in the center of the programmed temperature control box, the inlet gas path was connected below the coal sample tank, and the outlet gas path was connected above the coal sample tank. The temperature probe was placed in the center of the coal sample tank. The gas composition was collected and analyzed by gas chromatography. The inhibition rate is the percentage of the difference in the amount of CO produced by the coal samples before and after gel treatment at the same temperature and the ratio of the amount of CO produced by the raw coal samples. The calculation formula is:

$$\beta = \frac{A - B}{B} * 100\% \quad (2)$$

Where β is the inhibition rate of the gel for the coal, A is the amount of CO released from the raw coal sample at T temperature, ppm; B is the amount of CO released from the gel-added coal sample at T temperature, ppm.

3. Results and discussions

3.1. Gelation time and bonding degree

Following pre-experimental work, BCC-CMC solution with concentration of 2.5 % and 3 %, crosslinking agent with concentration of 20 % and 30 %, and pH modifier with concentration of 2.5 % and 3 % were selected. Under the premise of fixing the concentration of each of the three solutions of BCC-CMC, crosslinking agent, and pH modifier, the other two solutions were added according to the ratios, seven experimental group were carried out. The outcomes regarding experimental variables, proportions, gelation time and bonding degree are outline below:

Among, groups 1~3: the BCC-CMC concentration was 3 %, the crosslinking agent concentration was 20 %, and the GDL concentration was 2.5 %. Group 4: the BCC-CMC concentration was 3 %, the crosslinking agent concentration was 30 %, and the GDL concentration was 2.5 %. Group 5~6: the BCC-CMC concentration was 3 %, the crosslinking agent concentration was 20 %, and the GDL concentration was 2 %. Group 7: the BCC-CMC concentration was 2.5 %, the crosslinking agent concentration was 20 %, and the GDL concentration was 2.5 %.

Based on the experimental results, it can be concluded that keeping the concentration and dosage of BCC-CMC constant, along with the concentration of crosslinking agent and GDL, the gelling time decreases with increasing dosages of the crosslinking agent and GDL (groups 2, 3, 5, 6). Moreover, increasing the usage of GDL while maintaining other conditions constant (groups 1 and 3) also reduces gelation time. Conversely, with a constant crosslinking agent and GDL, the gelation time decreases as the concentration of BCC-CMC decreases (groups 3 and 7). Additionally, increasing the concentration of the crosslinking agent shortens the gelation time (groups 2 and 4). After filtering and weighing the bonded coal and crushed coal samples with a strainer, it was found that, at the same drying temperature, group 4 exhibited the highest bonding rate, reaching 70.72 %. Consequently, the coal bonded with the gel formed a cohesive unit, filling the gaps between coal samples and decreasing the surface area exposed to air, thereby lowering the risk of coal spontaneous combustion.

3.2. Viscosity test of BS-CMC gel

Through viscometer, to determine the most factors affect the viscosity of the gel by testing the viscosity of the gel. And to observe its

stability based on the results. The test results were as follows:

Fig. 3 illustrates that groups 5 and 6 exhibited superior performance with higher viscosity and greater stability at room temperature. Conversely, the viscosity of gels in groups 1~4 was lower, with group 7 displaying the lowest viscosity. Additionally, it is evident that the concentration of BCC-CMC primarily affects the viscosity of the gels, followed by the concentration of GDL, while the impact of the crosslinking agent is minimal.

Among these factors, when all other variables are held constant, the concentration of BCC-CMC has the greatest effect on the viscosity of the gel, followed by the concentration of GDL, while the concentration of crosslinking agent has a minor effect, and the combined amount of crosslinking agent and GDL has the least effect on the viscosity of the gel.

3.3. Performance testing of BS, BCC, BSC

3.3.1. XRD test of BS, BCC and BSC

The alteration in the crystal structure of BCC before and after preparation can be examined by XRD spectrum. Fig. 4 depicts the XRD patterns of BS, BCC and BSC.

Cellulose, hemicellulose and lignin constitute the primary components of bagasse. Cellulose possesses a crystal structure due to hydrogen bonding, while hemicellulose and lignin exhibit amorphous characteristics (Gond et al., 2021). Typical cellulose I exhibits a sharp diffraction peak at $2\theta = 22°$. BS exhibits peak near 16.48°, 22° and 34.56°, indicative of the typical cellulose I structure. The cellulose crystals exhibited characteristic attributes corresponding to the 101, 002, and 004 planes, respectively (Vanitjinda et al., 2019). BSC exhibited a prominent diffraction peak at 21.76°, along with weak diffraction peaks at 16.32° and 34.68°, which closely resemble the peak positions observed for BS.

In the case of BCC, the peak at 16° disappeared entirely, while a peak emerged at 20.08°, indicating the weakening of hydrogen bonds between the cellulose molecules and the disruption of the crystal structure (Chen et al., 2020). The Fig. 4 reveals that following the chemical reaction, the intensity of the original characteristic peaks of BCC either disappeared or diminished, and new carboxymethyl groups was introduced, resulting in alterations to the original cellulose crystal shape.

3.3.2. FTIR test of BS, BCC and BSC

Through FTIR, to study the chemical changes by identifying the functional groups present in the cellulose before and after treatment. The prepared BS and BCC were analyzed by FTIR spectroscopy, and the obtained curves are shown in Fig. 5.

Fig. 5 reveals broad bands in the wavenumber range between 3700

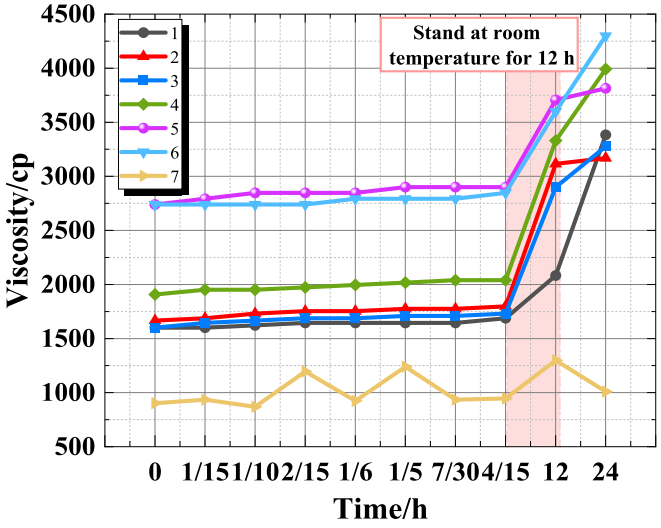

Fig. 3. Gel viscosity change with time.

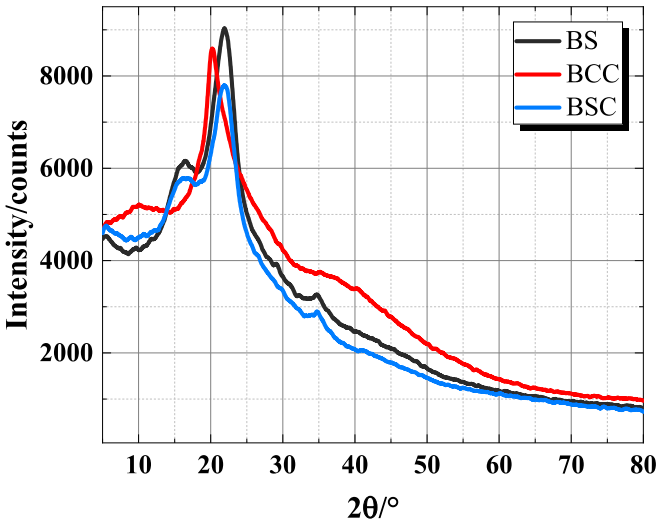

Fig. 4. X-ray diffraction pattern of BS, BCC and BSC.

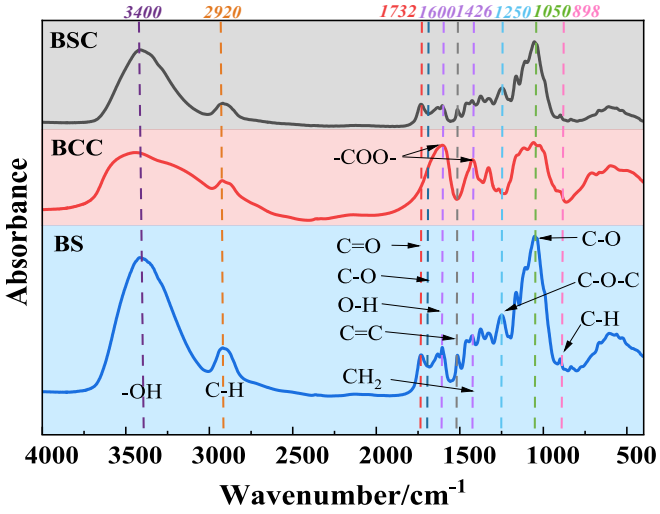

Fig. 5. FTIR of BS, BCC and BSC.

cm^{-1} and 3200 cm^{-1} for all samples, representing the O—H stretching vibrations in the phenolic hydroxyl and hydroxyl (—OH) groups within the cellulose structure, along with stretching vibrations of intermolecular and intramolecular hydrogen bonding. Compared to the BS raw material, BCC exhibited broader absorption peaks in this wavenumber range, suggesting weakened hydrogen bonding between BCC molecules and increased content of free hydroxyl groups (Chen et al., 2015). Characteristic peaks near 2920 cm^{-1} in all samples correspond to C—H stretching vibrations of methyl and methylene groups in the structure of cellulose, hemicellulose, and lignin. Characteristic peaks near 1328 cm^{-1} correspond to bending vibrations of C—H and C—O bonds in the aromatic rings of polysaccharides. The peak at 1600 cm^{-1} represents the bending vibration of the O—H bond in the adsorbed water. The band at 1426 cm^{-1} corresponds to the bending vibration of CH_2 in cellulose. The vibration near 1050 cm^{-1} corresponds to the C—O stretching of hemicellulose and lignocellulose, and the intensity of the BCC peak was weakened after the treatment, indicating that the content of hemicellulose and lignin was reduced after alkali treatment of cellulose. In addition, the C—C cyclic band at 1165 cm^{-1} and the C—O—C glycoside ether band at 1106 cm^{-1} are derived from the polysaccharide fractions. The band at 898 cm^{-1} corresponds to the stretching vibration of glycoside C—H outside the cyclic aromatic plane, represents a

characteristic of the β-glycoside bond and the amorphous form of cellulose, and which disappears progressively in BCC as a result of hydrolysis and molecular weight reduction.

In the FTIR spectra of mashed BS, the peak at 1732 cm^{-1} corresponds to the C═O stretching vibration of the acetyl and glucuronic acid ester groups in pectin, hemicellulose or the ester groups of the aromatic components in lignin and hemicellulose. Due to the removal of hemicellulose and part of lignin by chemical treatment, the peak disappeared in BCC. Similarly, the absorption peaks observed in the BS spectra 1635 cm^{-1} and 1465 cm^{-1} corresponds to the C═C stretching vibration of the lignin aromatic ring or the C—H bending of lignin and hemicellulose. In addition, BS showed a characteristic band at 1514 cm^{-1}, which due to the planar stretching vibration of the aromatic ring C═C in lignin, while the vibrational band at 1250 cm^{-1} corresponds to the C—O—C stretching vibration of the aryl–alkyl ether of lignin. In BSC, the intensity of these peaks mentioned above was reduced, indicating that the oxidase could not remove lignin completely. However these peaks were not present in BCC, which indicates that lignin can be completely removed from its structure.

FTIR results showed that most of the lignin and hemicellulose were removed from the BS structure after extraction. BCC showed a strong absorption peak at 1600 cm^{-1}, and the absorption peaks at there and 1426 cm^{-1} became wider, which was caused by the stretching vibration of —C═O in the carboxymethyl cellulose —CH_2COONa group, which is the symmetric and asymmetric stretching vibration absorption peak of —COO—, which indicates that the carboxylation occurs in BS (Gu et al., 2022; Yang and Chen, 2009). The peak near 1700 cm^{-1} comes from the C—O group of sodium hydroxyacetate, a by-product produced by the carboxymethyl cellulose process. This characteristic peak is not evident in the spectrum of carboxymethyl cellulose prepared in this experiment, indicating the by-product is essentially absent (Yang and Chen, 2009). It can be see that BCC was successfully separated and prepared from BS.

3.4. Gel thermal analysis

According to the results of viscosity test and gelation time, group 5 gels were analyzed by thermogravimetric experiment. Fig. 6 shows the thermal decomposition curve of the gel under nitrogen atmosphere.

From Fig. 6, it can be seen that the thermal decomposition of the gel mainly occurs in two stages: 30~260 °C and 260~550 °C. The weight loss in the first stage is mainly caused by the evaporation of free and bound water in the gel, the mass loss of the gel below 200 °C, which is about 8.92 %, with a maximum weight loss rate of 0.88 %/min, and the corresponding decomposition temperature is 81.6 °C. The weight loss in the second stage is due to thermal cleavage of the molecular chains of the gel itself, with a mass loss of 33.93 %, the maximum weight loss rate of 6.15 %/min, and the corresponding temperature is 285.7 °C.

From the data, it is not difficult to find that the gel has good thermal stability. When heated to 800 °C, the sample residual carbon is as high as 50.73 % when indicating that the gel material has high thermal stability, and high temperature will not affect its practical application.

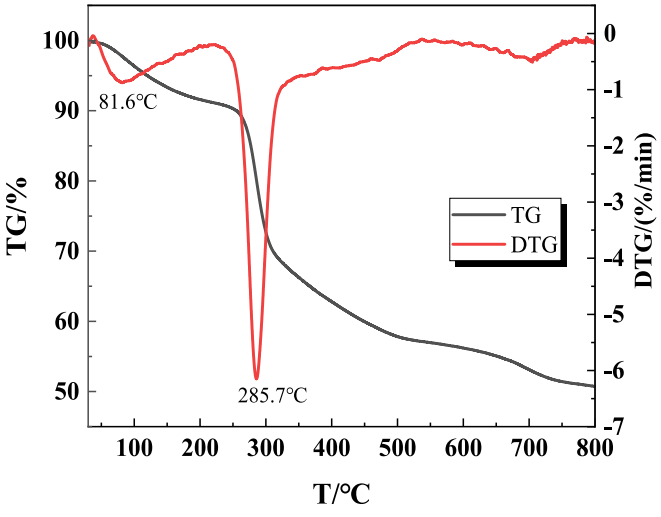

Fig. 6. TG-DTG curves of BCC-CMC gel.

3.5. Performance test of gel-added coal samples and raw coal samples

Mix the gels prepared in Table 2 with coal samples at a ratio of 1: 10, dried and ground them into 80-mesh powder. Then, the 7 groups of gel-added coal samples and raw coal samples with the same weight and mesh are tested by thermal analysis and functional groups testing. The gel-added coal samples were numbered as 1 + raw coal, 2 + raw coal, …, 7 + raw coal according to the ratio in Table 2.

3.5.1. Inhibition property analysis

The inhibition properties of the gel material in the spontaneous combustion process of coal were tested by conducting temperature programmed experiments on the raw coal samples and the gel-added coal samples, and observing the changes of the gas product concentration and the oxygen concentration at the outlet during the temperature programmed process. According to the previous experimental results, 5 + raw coal samples was selected for comparison with the raw coal. CO, CO_2, CH_4 and C_2H_4 was chosen as the index gas.

Fig. 7 illustrates the effect of gel on O_2 concentration during coal oxidation as a function of temperature. As the temperature continues to rise, the O_2 concentration at the outlet of both coal samples was decreasing, and the oxygen consumption rate was gradually accelerated. In the low-temperature stage, the oxygen consumption of both coal samples was low, and with the increase of temperature, the oxidation rate of coal was accelerated and the oxygen consumption gradually increased. Compared with the raw coal, the overall oxygen consumption of the gel-added coal samples was reduced, indicating that the gel has a certain inhibition effect.

Fig. 8(a) and Fig. 8(b) shows the change of CO and CO_2 produced during the heating of the raw coal sample and the gel-added coal sample over time. It can be seen that the trends of CO and CO_2 produced during the heating and oxidizing process are basically the same for both coal samples. In the low temperature stage, small amounts of CO and CO_2 were produced, and the concentration increase was slow. Large amounts of CO and CO_2 were produced above 190 °C and above 220 °C, increased exponentially. Compared with the raw coal, the CO and CO_2 concentrations of the gel-added coal samples were lower at the same temperature, which indicated that the gel had a significant inhibitory effect on the oxidation of coal. At 250 °C, the CO and CO_2 concentrations released from the raw coal samples were 6806 ppm and 22025 ppm, respectively, while those from the gel-added samples were 4729 ppm and 14687 ppm,

Table 2
Experimental variables and gelation time, bonding degree.

Groups	BCC-CMC dosage	Crosslinking agent amount	GDL usage	Gelation time	Bonding degree
1	20.07 g	10 %(2.0 g)	1.5 % (0.3 g)	7min25s	67.79 %
2	20.00 g	8 %(1.6 g)	2 %(0.4 g)	7min29s	65.14 %
3	20.03 g	10 %(2.0 g)	2.5 % (0.5 g)	7min25s	65.67 %
4	20.00 g	8 %(1.6 g)	1.5 % (0.3 g)	7min23s	70.72 %
5	20.00 g	8 %(1.6 g)	2 %(0.4 g)	7min21s	64.94 %
6	20.00 g	10 %(2.0 g)	2.5 % (0.5 g)	7min35s	66.60 %
7	20.00 g	10 %(2.0 g)	2.5 % (0.5 g)	6min32s	62.70 %

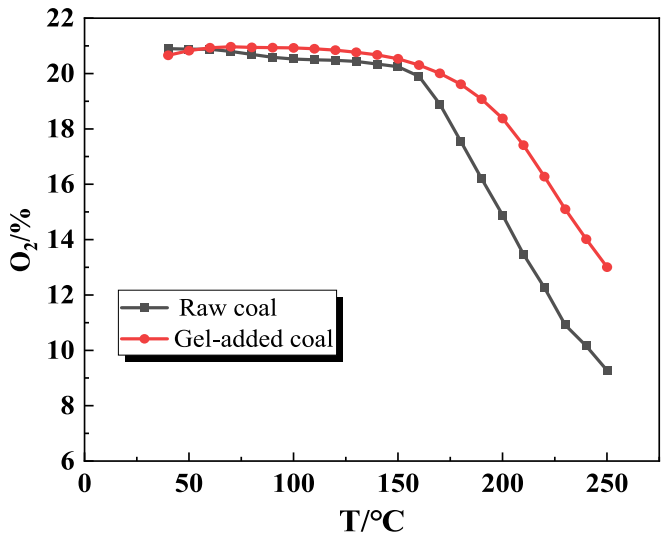

Fig. 7. O_2 concentration during the temperature-programmed oxidation of coal.

the CO inhibition ratio is calculated to be 30.5 %.

Fig. 8(c) shows the change of CH_4 produced during the heating of the raw coal sample and the gel-added coal sample over time. It can be seen from the curve in the figure that in the low temperature oxidation stage, the CH_4 concentration generated are all small, less than 150 ppm. With the increase of temperature, the CH_4 concentration generated in the raw coal increases exponentially. Compared with the raw coal, the CH_4 concentration in gel-added coal samples has been lower than that of raw coal, and the growth rate is lower than that of raw coal. Fig. 8(d) shows the change of C_2H_4 produced during the heating of the raw coal sample and the gel-added coal sample over time. It can be seen from the figure that the change trend of C_2H_4 concentration produced by the two coal samples during the heating process is the same. C_2H_4 was not produced during the low temperature process, and the concentration showed an increasing trend as the temperature increased. The critical temperature of C_2H_4 produced by the raw coal sample was 110 °C, while the critical temperature of the gel-added coal sample was 120 °C. When the temperature was increased to 250 °C, the C_2H_4 produced by the raw coal sample was 11.066 ppm, and the C_2H_4 produced by the gel treated coal sample was 8.589 ppm.

The addition of gel reduces the oxidation reaction rate of coal, inhibits the coal oxygen reaction process, and has a certain inhibitory effect on the oxidation spontaneous combustion process of coal.

3.5.2. *Analysis of the effect of gel on coal weight and heat*

Through TG-DTG, to analyze the gel's impact on the coal's spontaneous combustion process by comparing the mass changes of gel coal samples and raw coal samples during the heating process, and dividing the stage of coal spontaneous combustion by the mass change corresponding to the temperature point. The TG-DTG curves of raw coal samples and gel-added coal samples obtained from the experiments are shown in Fig. 9 and Fig. 10.

It can be seen from Fig. 9 and Fig. 10, the general change rule of the TG-DTG curves of the gel-added coal samples and the raw coal samples are similar. The mass changes produced by the coal samples in the process of spontaneous combustion were divided into four stages (Qin et al., 2014): stage I dehydration and weight loss stage, stage II oxygen absorption and weight gain, stage III thermal decomposition stage, stage IV combustion weight loss stage. This process consists of five various

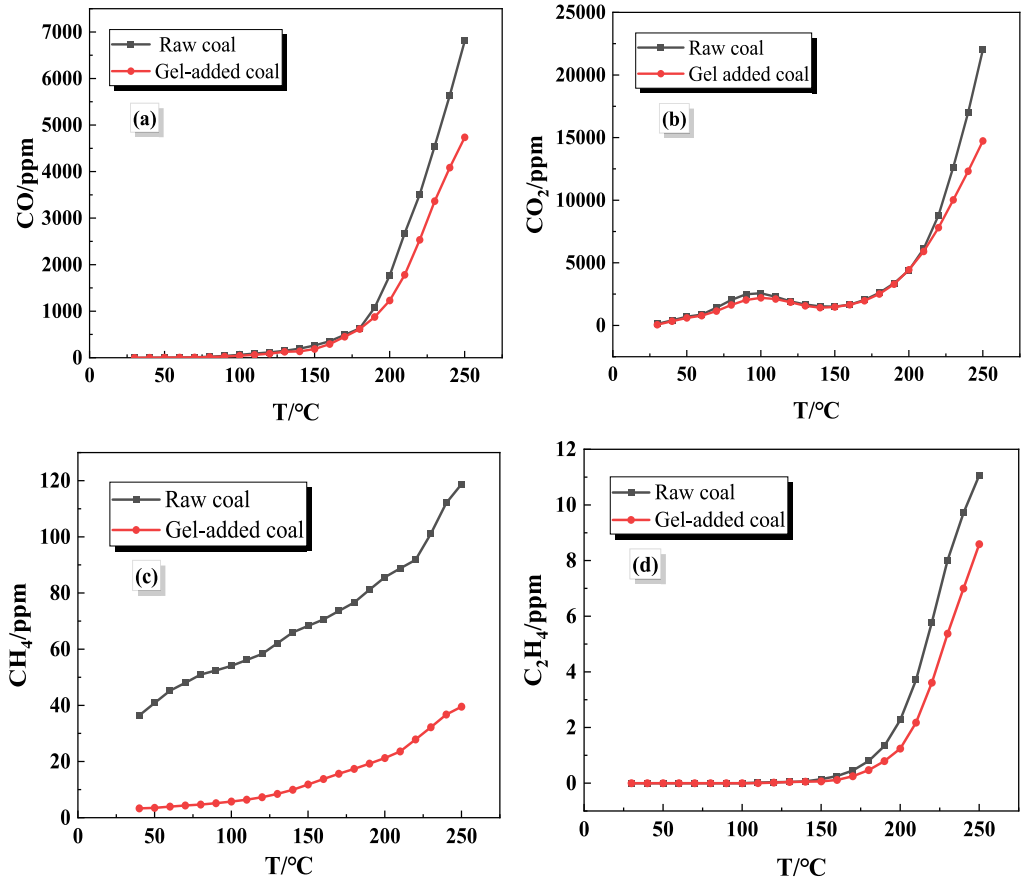

Fig. 8. The changes of the concentration of each gas component with time.

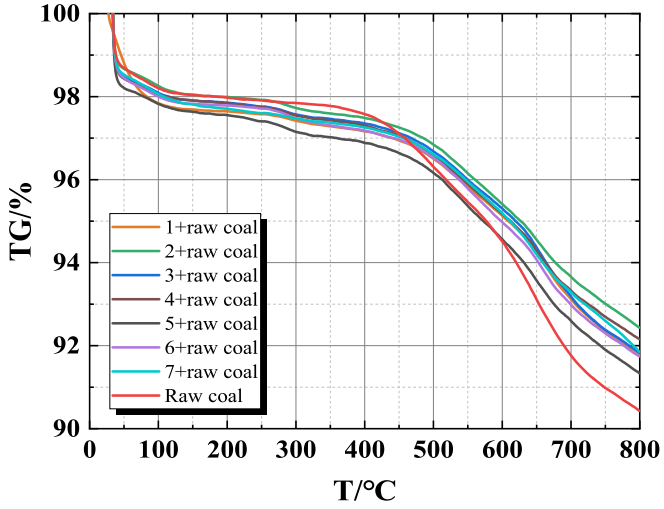

Fig. 9. TG diagram of raw coal samples and gel-added coal samples.

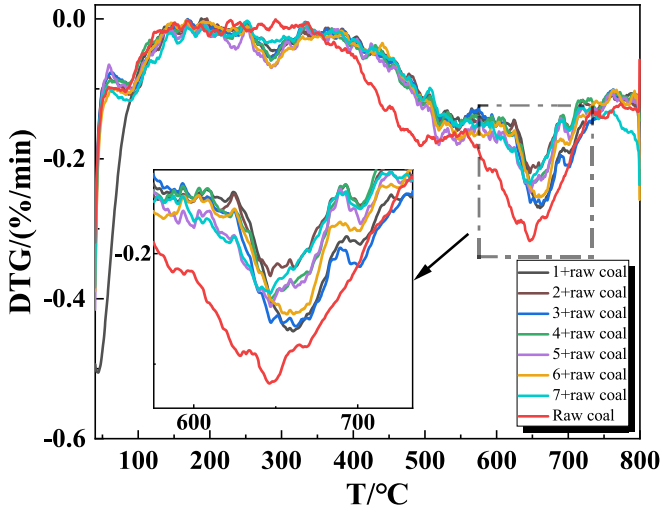

Fig. 10. DTG diagram of raw coal samples and gel-added coal samples.

characteristic temperatures (Dou et al., 2022; Xu et al., 2023) critical temperature (T1), drying temperature (T2), decomposition temperature (T3), ignition temperature (T4), and maximum mass loss temperature (T5). Take the TG-DTG curve of raw coal as an example, and mark these temperature points in Fig. 11. These characteristic temperatures are described as follows: the critical temperature is the temperature that appeared at the first maximum peak point of the weight loss rate. The drying temperature is the temperature at which the coal sample starts to rise due to the lowest water loss mass, that is, the temperature at the first minimum mass loss rate on the TG curve. When the coal reaches the decomposition temperature, the amount of oxygen adsorption and the mass loss caused by the oxidation of coal reaches a balance, will enter a relatively fast weightless stage. The ignition temperature is the temperature at which the coal sample starts to burn, which is obtained by extrapolation temperature method. The maximum mass loss temperature is the peak DTG temperature. The characteristic temperature points of each coal samples are shown in Table 3.

As can be seen from Fig. 11, (1) in the dehydration and weight loss stage (30~180 °C), due to the increasing temperature, the water in the coal samples began to evaporate, and the volatile gases escaped from the gap. The TG curve began to decline, the DTG curve appeared a weight loss peak, and the quality of the coal samples began to decline. (2) In the stage of oxygen absorption and weight gain (180~350 °C), as the

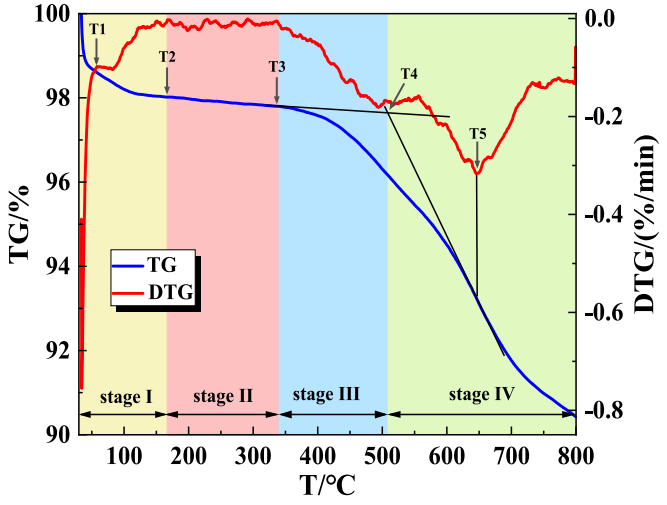

Fig. 11. TG-DTG curve of raw coal samples during heating process.

Table 3
Characteristic temperatures of raw coal and gel-added coal samples.

Coal samples	T1/°C	T2/°C	T3/°C	T4/°C	T5/°C	ΔTG_I/%
Raw coal	58.3	166.8	336.8	508.3	645.7	1.98
1 + raw coal	71.9	172.4	350.9	547.5	660.4	2.34
2 + raw coal	59.7	168.2	347.2	510.2	647.2	1.99
3 + raw coal	61.2	171.2	351.2	521.1	653.7	2.11
4 + raw coal	61.8	170.8	350.3	518.1	646.8	2.11
5 + raw coal	59.7	168.2	343.1	512.2	646.7	2.41
6 + raw coal	68.3	170.8	385.3	529.3	656.8	2.19
7 + raw coal	61.1	171.6	337.6	520.6	647.2	2.19

temperature of the coal sample continues to rise, the adsorption of oxygen on the coal dominates, the oxygen adsorbed on the surface of coal increases and generates intermediate complexes, making the adsorption of oxygen on the coal greater than the escape of gas. The TG curve rises slightly, the quality of the coal sample increases slowly, the DTG curve at about 290 °C appears to be the maximum, which indicates that the mass increase rate of coal samples is the fastest at this temperature. (3) In the thermal decomposition stage (350~510 °C), before 400 °C, the weight loss of coal samples is not obvious. With the further increase of temperature, the coal samples enter the thermal decomposition stage, and there are obvious mass changes. (4) Combustion weight loss stage (>520 °C), with the continuous increase of temperature, the coal sample undergoes a violent combustion reaction and generates a large amount of gas and heat. The weight loss rate of the coal samples increased rapidly, indicating that the coal spontaneous combustion entered the auto-oxidation accelerated stage, and the weight loss of the coal samples was obvious, and reached a larger value in this stage at 556 °C. Then the weight loss rate showed a decreasing trend, and reached the maximum weight loss rate at about 650 °C. Until the end of the coal combustion, the quality no longer changed, and the quality of the coal samples was basically unchanged.

As shown in Table 3, compared with the raw coal the characteristic temperature of the coal samples treated by the gel has increased to different degrees. For example, T1 and T2 of the first group of gel-added coal samples have increased by 13.6 °C and 5.6 °C respectively, indicating that the gel has good water retention. By calculating the mass change in the dehydration and weight loss stage, that is ΔTG_I, it can be found that the gel loses water first in the heating process, which makes the gel-added coal sample lose weight faster. The mass change rate of the gel-added coal sample in group 1 was 2.34 %, while that of the raw coal sample was 1.98 %, indicating that the gel inhibited the low-temperature oxidation of coal to some extent. In the low-temperature

oxidation stage, the gel lost water and took away the heat of the gel-added coal samples at the same time, which makes the gel-added coal samples appeared later than the raw coal samples in the oxygen absorption and weight gain stage and thermal decomposition stage. With the increase of temperature, the aromatic structure of coal was destroyed, and the mass loss rate was accelerated, reaching the maximum mass loss temperature (T5). Compared with raw coal, the T5 temperature of gel-added coal samples increased significantly, indicating that gel has high-temperature flame retardant effect.

3.5.3. Fourier transform infrared spectroscopy analysis

Microstructure is the fundamental cause of the variability of coal spontaneous combustion. Through FTIR to reflect the gel's impact on the coal's spontaneous combustion by comparing the functional groups change of gel coal sample and raw coal samples. The FTIR characterization results of raw coal samples and gel-added coal samples are shown in Fig. 12.

The peak changes of functional groups in different wavenumber ranges of the gel-added coal samples and the raw coal samples are shown in Fig. 12. The wavenumber range of 3750~3150 cm^{-1} represents the hydroxyl group (—OH) stretching vibration interval. It can be seen from the figure that the stretching vibration of —OH of the coal sample with gel is weaker than that of the raw coal, indicating that the active group (i.e., hydroxyl content) of the coal sample added with gel is reduced, and the oxidation activity is lower than that of the raw coal. 3100~2800 cm^{-1} represents the stretching vibration interval of aromatic and aliphatic C—H. The peaks of functional groups in this interval are mainly those of methyl and methylene group. The aliphatic C—H component reacts with oxygen and generates various oxygen-containing functional groups. Compared with the raw coal, the content of aliphatic C—H component in the coal samples added with gel is higher than that of the raw coal, which means that the amount of oxygen-containing functional groups generated by the coal samples added with gel is less than that of the raw coal. The —COOH of the coal samples added with gel was weaker than that of the raw coal at 2400~2300 cm^{-1}, indicating that the addition of gel inhibited the conversion of aliphatic groups to carboxymethyl intermediates (Wang et al., 2020). The stretching vibration interval of carbonates and aromatic hydrocarbons (C═O) was at 1700~1500 cm^{-1}. In this interval, the stretching vibration peaks of the coal samples added with gel were weaker, indicating that the gel inhibited the oxidation reaction of the coal. 1460~1435 cm^{-1} represents the vibration peak of methyl antisymmetric deformation, which is the position of the aliphatic peaks, which indicates that the raw coal sample and the treated coal sample contain $—CH_2$ and $—CH_3$ functional groups. 1150~950 cm^{-1} represents the C—O stretching vibration range of alcohols, phenols and ethers, and all showed strong absorption peaks. The peaks of the raw coal in the wavenumber range changed significantly. Compared with the raw coal, the coal samples added with gel showed different degrees of weakening, indicating that the gel can effectively inhibit the conversion of aliphatic groups to carboxyl intermediate products in the coal samples. 950 cm^{-1}~500 cm^{-1} represents the C—H out-of-plane bending vibrational range of the olefins and aromatic hydrocarbons.

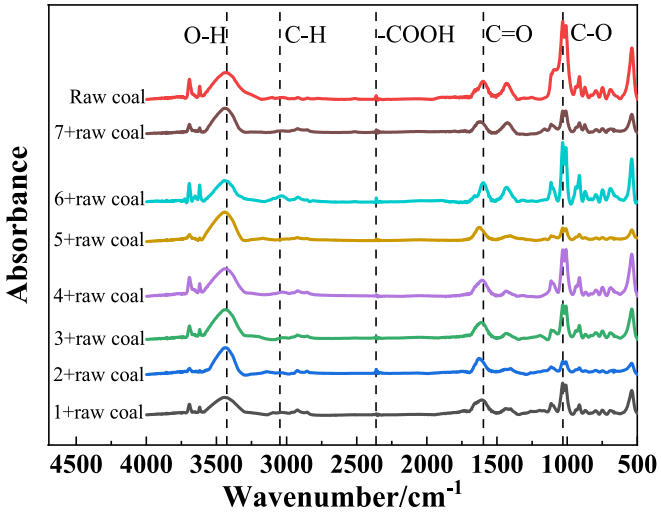

Fig. 12. FTIR diagram of gel-added coal samples and raw coal samples.

Overall, the aliphatic C—H components and C═O- containing compounds play a major role in the spontaneous combustion process of coal, and C—H reacts with oxygen to form oxygen-containing functional groups. After gel treatment, the absorption peaks of C—H is enhanced, and the absorption peaks of C═O is weakened, indicate that the gel can inhibit the spontaneous combustion oxidation of coal, and reduce the possibility of coal spontaneous combustion.

3.6. Inhibition mechanism

As can be seen from the abovementioned experimental results, the prepared gel can play an effective inhibitory role in both the low temperature oxidation and high-temperature decomposition stages of coal. The specific mechanism is as follows.

3.6.1. Physical inhibition mechanism

BCC-CMC solution is liquid before gelation, and BCC and CMC are hydrophilic and film-forming. When BCC-CMC gel contacts with coal, it can wet coal for a long time and form a liquid film on the surface of coal. The liquid film can isolate the contact between coal and oxygen and reduce the oxidation heat release rate of coal. Coal spontaneous combustion generally occurs in loose coal, which has a large number of pores and cracks. BCC-CMC gel has a certain viscosity and fluidity, which can be filled in pores and cracks, so that oxygen cannot penetrate into the coal, block the air leakage channel, and reduce the contact between coal and oxygen. When the temperature increases, the water in the gel reduces the temperature of the coal body by absorbing heat, and the temperature of the high-temperature coal body is reduced under the combined action of plugging and heat absorption (See Fig. 13).

3.6.2. Chemical inhibition mechanism

The nature of coal spontaneous combustion is a process that various free radicals in coal molecules react with oxygen in the air to generate a large number of oxidation products (such as CO, CO_2, etc.) and release heat, as shown in the Fig. 14. With the increase of temperature, some chemical bonds between coal molecules are broken, a large number of carbon free radicals (R•) are generated (Xi et al., 2022). Carbon radicals react with oxygen to form peroxide free radicals (ROO•), which are strongly oxidizing and extremely unstable, and form peroxides (ROOH) by capturing H (Xi et al., 2021). As the temperature continues to rise, ROOH is decomposed into alkoxy radicals (RO•) and hydroxyl free radicals (•OH). With the continuous increase of coal temperature, RO• reacts with oxygen to form C═O, which reacts with •OH to form carbonyl free radicals (C═O•), which thermally decomposed to release CO and generate new R•. Part of C═O further reacts with O_2 to form —COO— (Yan et al., 2021), and then reacts with •OH to form carboxyl free radicals (COO•), decomposed by heat to release CO_2 and other gases. These newly generated R• continue to participate in the oxidation reaction, and this process is repeated, producing more free radicals and releasing a lot of heat.

For untreated coal samples, as the temperature rises, C—H in coal reacts with oxygen to produce oxygen-containing functional groups such as C—O, C═O, —COO—, accompanied by the production of gases such as CO and CO_2. As BCC-CMC contains a large number of hydroxyl groups, it can absorb the heat generated in the oxidation reaction of coal and reduce the temperature of the coal itself. At the same time, BCC-CMC gels can be attached to the surface of the coal body to isolate the

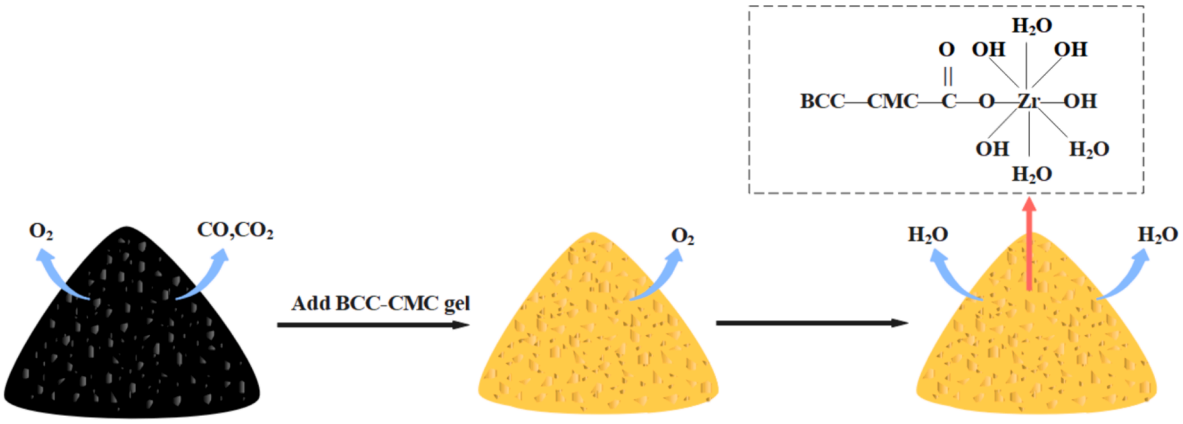

Fig. 13. The physical inhibition mechanism of BCC-CMC gel.

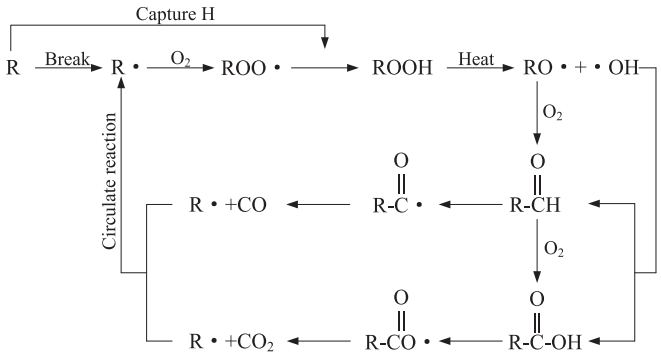

Fig. 14. The inhibition mechanism of BCC-CMC gel.

contact between oxygen and coal, thus interrupting the chain cycle reaction of coal. Therefore, the contents of oxygen-containing functional groups C═O and —COO— in the gel-treated coal samples was reduced, which also led to the reduction of CO and CO_2 content produced in the thermal decomposition.

4. Conclusion

In this work, a gel material with good thermal stability and flame retardant effect was prepared, from which BCC-CMC used as substrate, zirconium citrate as cross-linking agent, and GDL as pH modifier. The gelation time and flame retardant properties of the gel were studied. The main conclusions are as follows:

BCC was successfully extracted from BS, and the prepared gels were adhesive and blocking. XRD and FTIR were performed on the prepared BS and BCC, and the results showed that carboxylation reaction occurred in the treated BCC, and there were basically no by-products. BCC-CMC gel can effectively plug the cracks on the surface of coal, and inhibit coal spontaneous combustion by reducing the contact between coal and oxygen.

The temperature programmed experiments showed that the inhibition effect of the gel was remarkable. Compared with raw coal, the CO inhibition rate of the gel-added coal samples was 30.5 % at 250 °C. The addition of gel effectively reduced the reaction rate of coal spontaneous combustion and inhibited the oxidation process of coal.

TG-DTG results showed that the characteristic temperature points of the coal samples with the addition of gel were higher than those of the original coal samples, which indicated that the gel had excellent inhibition performance for the coal samples. FTIR results showed that the gel could reduce the content of hydroxyl and other reactive functional groups in the coal samples, which could play the role of moisturizing and cooling in the low-temperature stage of coal spontaneous combustion, and prevent the oxidation cyclic reaction of the coal in the high-temperature stage to inhibit the spontaneous combustion of the coal process.

CRediT authorship contribution statement

Xiaowei Geng: Methodology, Conceptualization. **Yuanyuan Feng:** Writing – original draft, Validation, Investigation, Data curation. **Yinhui Wang:** Resources. **Hemeng Zhang:** Resources. **Yujiao Liu:** Supervision. **Ke Gao:** Writing – review & editing, Supervision, Resources, Project administration, Funding acquisition.

Declaration of competing interest

The authors declare that they have no known competing financial interests or personal relationships that could have appeared to influence the work reported in this paper.

Data Availability

All relevant data are within the paper.

Acknowledgements

The authors greatly acknowledge the financial support by the National Natural Science Foundation of China (No.52074148, 52104194, 52274205), University-local government scientific and technical cooperation cultivation project of Ordos Institute-LNTU, (YJY-XD-2023-012). There was no additional external funding received for this study.

References

Beh, J.H., Lim, T.H., Lew, J.H., Lai, J.C., 2020. Cellulose nanofibril-based aerogel derived from sago pith waste and its application on methylene blue removal. Int. J. Biol. Macromol. 160, 836–845.

Chang, X.G., Cao, X.S., Xiao, L.X., Li, B.Y., Wu, R.C., 2024. Preparation and adsorption properties of bagasse cellulose based carbon aerogel. New Chem. Mater. 52 (04), 212–216. +222.

Chen, J., Li, H., Fang, C.Q., Cheng, Y.L., Tan, T.T., Han, H.Z., 2020. Synthesis and structure of carboxymethylcellulose with a high degree of substitution derived from waste disposable paper cups. Carbohydr. Polym. 237, 116040.

Chen, Y., Wei, Q.M., Yang, J.T., Zhu, W.R., Yu, G.Y., Huang, Z.Q., 2015. Preparation and characterization of carboxymethyl cellulose from mechanically activated bagasse cellulose. Trans. Chin. Soc. Agric. Eng. 31 (23), 300–307.

Chen, P.Y., Zhou, C.S., 2023. Study on fire preventing and extinguishing characteristics of mine-used dual network gel. Saf. Coal Mines 54 (11), 84–91.

Deng, J., Yang, N.N., Wang, C.P., Chen, G.H., Kang, F.R., Ren, L.F., Cui, X.C., Bai, G.X., 2022. Key technology of "preventing-suppressing-extinguishing" coordinated fire preventing and extinguishing for coal spontaneous combustion in goaf. Saf. Coal Mines 53 (9), 1–8.

Ding, C., Li, Z.X., Wang, J.R., Lu, B., Gao, D.M., 2023. Effects of inert gas CO_2/N_2 injection on coal low-temperature oxidation characteristic: experiments and simulations. Arab. J. Chem. 16 (2), 104510.

Dong, K.L., Wang, J.F., Liang, Z.W., Shi, Q., 2020. Characteristics of CMC/ZrCit/GDL fire extinguishing gel used for mines. China Saf. Sci. J. 30 (1), 114–120.
Dong, K.L., Wang, J.F., Zhang, Y.L., Liang, Z.W., Shi, Q., 2022. Performance of fire extinguishing gel with strong stability for coal mine. Combust. Sci. Technol. 194 (8), 1661–1677.
Dou, G.L., Liu, J., Jiang, Z.W., Jian, H.D., Zhong, X.X., 2022. Preparation and characterization of a lignin based hydrogel inhibitor on coal spontaneous combustion. Fuel 308, 122074.
Fan, S.L., Zhou, J.R., Zhang, Y.J., Feng, Z.F., Hu, H.Y., Huang, Z.Q., Qin, Y.B., 2020. Preparation of sugarcane bagasse succinate/alginate porous gel beads via a self-assembly strategy: improving the structural stability and adsorption efficiency for heavy metal ions. Bioresour. Technol. 306, 123128.
Farid, E., Kamoun, E.A., Taha, T.H., El-Dissouky, A., Khalil, T.E., 2022. PVA/CMC/attapulgite clay composite hydrogel membranes for biomedical applications: factors affecting hydrogel membranes crosslinking and bio-evaluation tests. J. Polym. Environ. 30 (11), 4675–4689.
Gao, K., Qi, Z.P., Jia, J.Z., Li, S.N., Liu, Z.Y., Liu, Z.M., 2022. Investigation of coupled control of gas accumulation and spontaneous combustion in the goaf of coal mine. AIP Adv. 10 (4), 045314.
Gond, R.K., Gupta, M.K., Jawaid, M., 2021. Extraction of nanocellulose from sugarcane bagasse and its characterization for potential applications. Polym. Compos. 42 (10), 5400–5412.
Gu, F., Ma, J.X., Che, C.B., 2022. Preparation and structural characterization of carboxymethyl cellulose from corn stalk. J. Chin. Cereals Oils Assoc. 37 (09), 240–245.
Guo, Q., Ren, W.X., Zhu, J.T., Shi, J.T., 2019. Study on the composition and structure of foamed gel for fire prevention and extinguishing in coal mines. Process Saf. Environ. Prot. 128, 176–183.
Huang, Z.A., Wang, G.H., Zhang, Y.H., Yin, Y.C., Hu, X.M., Gao, Y.K., Yang, Y.F., Xin, H. H., 2022. Inhibition characteristics of a novel PAM/SA-Ca(OH)2 composite inhibitor to control coal spontaneous combustion. Fuel 314, 122750.
Jia, J.Z., Shan, S.W., Jia, P., Song, H.L., 2024. Chemical reaction process and dynamic characteristics of urea pyrolysis products in inhibiting gas explosion. Arab. J. Chem. 17 (6), 105813.
Kim, H.S., Kim, D.-W., Park, I.-S., Hong, H.-J., 2023. Adsorptive recovery of rare earth elements from aqueous solution by citric acid crosslinked carboxymethylated cellulose nanofibril aerogel. J. Clean. Prod. 418, 138189.
Li, S.L., 2018. Preparation of superabsorbent gel by modified sodium carboxymethyl cellulose. Coal Technol. 37 (11), 362–364.
Li, S.L., Zhou, G., Wang, Y.Y., Jing, B., Qu, Y.L., 2019. Synthesis and characteristics of fire extinguishing gel with high water absorption for coal mines. Process Saf. Environ. Prot. 125, 207–218.
Liu, D., Wang, J.P., Zhou, G., Jiang, W.J., Duan, J.J., Tian, F.C., Xu, H.Z., 2021. Synthesis and performance analysis of new hybrid polymer gel based on carboxymethyl cellulose for preventing spontaneous coal combustion. ChemistrySelect 6 (26), 6661–6670.
Ma, Y.M., Miao, S.Y., 2023. Study on water absorption of sodium carboxymethylcellulose gel. Chem. Reagents 45 (10), 77–82.
Markeb, A.A., Moral-Vico, J., Sánchez, A., Font, X., 2023. Optimization of lead (II) removal from water and wastewater using a novel magnetic nanocomposite of aminopropyl triethoxysilane coated with carboxymethyl cellulose cross-linked with chitosan nanoparticles. Arab. J. Chem. 16 (8), 105022.
Qiao, M., Ren, T., Roberts, J., Yang, X.H., Li, Z.B., Wu, J.M., 2022. New insight into proactive goaf inertisation for spontaneous combustion management and control. Process Saf. Environ. Prot. 161, 739–757.
Qin, R.X., Pang, W.H., Tao, Y., 2014. Effect of TG experimental conditions on the oxidative combustion characteristics of coal. J. Saf. Sci. Technol. 10 (05), 154–158.
Ren, W.X., Guo, Q., Zuo, B.Z., Wang, Z.F., 2016. Pressure balanced fire prevention and control technology during equipment withdrawing period of coal mining face in easy spontaneous combustion contiguous seams group. Coal Sci. Technol. 44 (10), 48–52. +94.
Ren, X.F., Hu, X.M., Cheng, W.M., Bian, S.S., Zhao, Y.Y., Wu, M.Y., Xue, D., Li, Y.S., Lu, W., Wang, P., 2020. Study of resource utilization and fire prevention characteristics of a novel gel formulated from coal mine sludge (MS). Fuel 267, 117261.
Rong, X.L., Cui, B., Huang, Q.M., Cui, M.J., Cheng, H., Feng, J., Huang, W.Y., 2022. Study on preparation of bagasse cellulose based carbon aerogels and their adsorption properties. Inorg. Chem. Ind. 54 (09), 126–135.
Shi, L.Z., Gao, K., Liu, Y.J., Shang, W.T., 2024. Effect of the periodic air leakage on spontaneous combustion in the gob of coal mine. Case Stud. Therm. Eng. 55, 104082.
Si, J.H., Zhao, Z.H., Li, L., Cheng, G.Y., Chen, J.C., 2024. Optimization of CO_2/N_2 injection ratios in goaf by saturation adsorption capacity. Arab. J. Chem. 17 (6), 105804.
Vanitjinda, G., Nimchua, T., Sukyai, P., 2019. Effect of xylanase-assisted pretreatment on the properties of cellulose and regenerated cellulose films from sugarcane bagasse. Int. J. Biol. Macromol. 122, 503–516.
Wang, J.F., Dong, K.L., Liang, Z.W., Zhao, Y.F., 2020. Study on preparation and characteristics of mine fire extinguishing gel. Saf. Coal Mines 51 (10), 126–130.
Wang, Y.Z., Dong, K.L., Zhang, Y.L., Dong, Z.Y., Wang, J.F., 2023. Study on preparation and characteristics of CMC/ZrCit/GDL fire-fighting gel foam. Coal Sci. Technol. 51 (6), 122–129.
Wang, K.S., Lu, W., Du, Y.F., Zhang, Q.S., Xu, J., 2016. Study on plastic water glass gel for preventing coal spontaneous combustion. Min. Saf. Environ. Prot. 43 (1), 8–11.
Wang, Y., Shi, D.W., 2022. In vitro and in vivo evaluations of nanofibrous nanocomposite based on carboxymethyl cellulose/polycaprolactone/cobalt-doped hydroxyapatite as the wound dressing materials. Arab. J. Chem. 15 (11), 104270.
Wang, L.J., Wang, J.R., Zhang, X., Guo, X.Y., 2019. Study on slurry diffusion law of high level drilling grouting fire prevention and control in goaf. China Saf. Sci. J. 29 (10), 71–77.
Wang, M. L., 2018. A method for preparing sodium carboxymethyl cellulose from straw. Guangdong Province. CN104894185B.
Xi, Z.L., Jin, B.X., Shan, Z., 2021. Reaction mechanisms involving peroxy radical in the low-temperature oxidation of coal. Fuel 300, 120943.
Xi, Z.L., Li, M.M., Li, X., Lu, L.P., Wang, J.W., 2022. Reaction mechanisms involving the hydroxyl radical in the low-temperature oxidation of coal. Fuel 314, 122732.
Xu, X.X., Yuan, S.J., Li, J.H., Guo, S.L., Yan, Z., 2023. Preparation of lignin-based intumescent nanogel and its mechanism of inhibiting coal spontaneous combustion. Energy 275, 127513.
Yan, B.R., Hu, X.M., Cheng, W.M., Zhao, Y.Y., Wang, W., Liang, Y.T., Liu, T.Y., Feng, Y., Xue, D., 2021. A novel intumescent flame-retardant to inhibit the spontaneous combustion of coal. Fuel 297, 120768.
Yang, Y., Chen, H.Z., 2009. Preparation of carboxymethylcellulose from steam exploded crop straw. CIESC J. 60 (07), 1843–1849.
Yuan, L., Wang, E.Y., Ma, Y.K., Liu, Y.B., Li, X.L., 2023. Research progress of coal and rock dynamic disasters and scientific and technological problems in China. J. China Coal Soc. 40 (05), 1825–1845.
Zeng, J., Li, Y., Li, J.R., Chen, R.R., Ping, Z.H., Ma, N.F., 2019. Preparation and properties of bagasse cellulose/CMC composite hydrogels. J. Cellul. Sci. Technol. 27 (04), 40–45.
Zhang, P., Liao, W.Y., Kumar, A., Zhang, Q., Ma, H.Y., 2020. Characterization of sugarcane bagasse ash as a potential supplementary cementitious material: comparison with coal combustion fly ash. J. Clean. Prod. 277, 123834.
Zhao, C.R., 2022. Study on New Colloid Material and Its Characteristics for Prevention and Extinguishment of Coal Spontaneous Combustion. Taiyuan University of Technology.
Zhu, H.Q., Hu, C., Zhang, Y.B., Hu, L.T., Yuan, X.L., Wang, X.K., 2020. Research status on prevention and control technology of coal spontaneous fire in China. Saf. Coal Mines 51 (3), 88–92.